Journal of Oil Palm Research Vol. 37 (1) March 2025 p. 110-121
DOI: https://doi.org/10.21894/jopr.2023.0063

ANALYSIS OF THE ENERGY CONSUMPTION OF MOTORISED CIRCULAR SAW WHEN CUTTING OIL PALM FROND

SUN QUN[1]* and ZAIDI MOHD RIPIN[1]

ABSTRACT

Existing pruning technique uses the sickle or chisel, manually or mechanically powered using small internal combustion engine. The current challenge of going for zero carbon emission for the oil palm industry requires the replacement of all internal combustion engines with battery powered electrical tools. It is important to reduce the force and power consumption of the cutting process which can affect the number of cuts made per battery charge. One efficient cutting process is the use of a circular saw which is widely adopted in the lumber processing but not in the oil palm harvesting. Cutting the oil palm fronds with a circular saw has never been studied before. In the paper, the mechanism of energy consumption in the circular saw-cutting process of oil palm fronds is studied, and the model of power (w) and work (J) is established. Comparing the test results with the theoretical values calculated by the model, indicating that no significant difference in cutting work model for the oil palm fronds ($38<F<145$, $0.72<R^2<0.91$, $P<0.05$) based on the different cutting conditions. The validated cutting energy equation is used in the optimisation of the cutting process of a 100 mm base wide of an oil palm frond resulting in the minimum cutting energy of 330 J for rotational speed of 1,000 rpm and feed rate of 10 mm/s.

Keywords: cutting force, energy consumption model, friction, frond, oil palm.

Received: 15 April 2023**; Accepted:** 3 October 2023**; Published online:** 5 December 2023.

INTRODUCTION

Oil palm is an important economic crop covering large swathes of arable land in Southeast Asia, Africa, South America and now extending to southern China. It contributed significantly to the world edible oil market (Meijide *et al.,* 2017). The integration of circular saw cutting in oil palm harvesting brings forth a range of benefits. Firstly, it improves efficiency by enabling faster and more precise cutting, leading to increased productivity and reduced labour requirements. Secondly, the precise and controlled cutting action of the circular saw minimises damage to the fronds, ensuring higher-quality harvested produce. Moreover, by optimising cutting parameters and implementing energy-efficient practices based on power consumption models, the overall cost of harvesting can be significantly reduced. This reduction in costs translates into improved profitability for farmers and greater competitiveness in the global market.

Maintenance of the tree requires periodical pruning of the fronds typically done as part of the harvesting of the oil palm fruit bunch (Jasim *et al.,* 2017). Research in the mechanics of cutting of oil palm fronds covered the effect of cutting angle and frond maturity on the specific reaction force and the energy requirement using spring assisted sickle (Jelani *et al.,* 1998) and normal sickle (Jelani *et al.,* 1999). Another cutting study was conducted on the chopping of empty fruit bunches, where it was shown that increasing the peripheral cutting speed increased the cutting power (Suryanto *et al.,*

[1] School of Mechanical Engineering,
Universiti Sains Malaysia (USM),
14300 Nibong Tebal, Penang, Malaysia.

* *Corresponding author e-mail: Sq842943050@outlook.com*

2009). All these were experimentally based and no cutting power model was developed. In order to improve the cutting performance of the current harvester tools, a cutting model is needed. The process of cutting with a spring-assisted sickle may involve some degree of energy wastage. A portion of the force applied to the spring may be absorbed or converted into other forms of energy instead of being entirely transmitted to the stalk for cutting. This can lead to decreased efficiency and necessitate a greater amount of energy to accomplish the same task. Spring-assisted sickles possess a more complex structure, including the spring mechanism, compared to circular saw cutting method. This potentially increases the costs and workload associated with maintenance. If the spring becomes damaged or malfunctions, repair or replacement is required, adding additional time and resource costs.

There is limited research on using circular saws for cutting oil palm fronds. However, there have been numerous research achievements in using circular saws for cutting other plants, which have significantly improved efficiency. The knowledge gained from research on circular saws in cutting other plants can be applied to the context of oil palm leaf stalks. Although there may be variations in the physical properties and cutting requirements of different plant species, the principles and insights gained from previous studies can serve as valuable references for developing efficient cutting methods for oil palm fronds. Meng (2018) described a method of an explicit kinetic simulation and experimental study of circular saw cutting system of mulberry cutting machine and carried out the orthogonal simulation for the optimisation of the combinations of operating parameters of the circular saw in cutting dynamic parameters. Li *et al.* (2022) studied the circular saw cutting force of apple branches and showed that cutting speed and the branch diameter had a significant effect on the cutting force, while the sawtooth number had a small effect on the cutting force. Abbood *et al.* (2018) studied three different cutting angles and their effect on cutting time. A randomised complete block design with three replications was used in the experiment. The results showed that 45° cutting angle was superior in obtaining the shortest time of frond cutting is 4.30 s. Jasim *et al.* (2017) evaluated the effects of motorised vibration cutters on some operational characteristics used for date palm fronds which indicated that the solution found in the oil palm harvesting can be readily applied to date palms. Abbood (2020) showed that frond strength influences the frond chopping force in particular the cutting angle. Eliçin *et al.* (2019) studied the cutting of grapes vines and determined that the cutting force and energy values increased with increasing knife-cutting angle from 0°-40°. The maximum cutting force, cutting strength, cutting energy and specific cutting energy was observed at 0° cutting angle as 319.3 N, 11.30 MPa, 2.393 N and 0.08464 J mm^{-2} respectively. On the modelling front, the theoretical sawing power of a circular saw was calculated by (Gao, 2016). Chu (2017) showed that the cutting work and the effect of rotational speed, feed rate and the inclination angle. Dong (2017) researched the single-factor tests to study the feed rate of the header, rotation speed, the inclination angle of the disc cutter and the diameter of the straw. Xie (2019) discussed the research on the optimisation of cutting parameters of sugarcane. It is clear that the theoretical modelling of the cutting process is an important part of the minimisation of the cutting force and power.

Circular saw cutting has emerged as a powerful tool for enhancing efficiency and quality in oil palm harvesting. By understanding the dynamics of circular saw cutting on oil palm fronds and establishing reliable power consumption models, we can unlock the full potential of this technique. The adoption of circular saw cutting in oil palm harvesting offers numerous advantages, including increased efficiency, improved quality, cost reduction, and reduced labour requirements. By embracing this innovative approach, the oil palm industry can achieve sustainable and profitable growth while meeting the rising global demand for this valuable crop. The paper shows the development of the model for the cutting power and work parameters of circular saw used in the cutting of the oil palm fronds. These cutting parameters are compared with the measured values obtained from cutting test bench to verify the accuracy of the model. To the best knowledge of the authors, the cutting model of a cutting power of a circular saw on the oil palm fronds has never been reported before. The industrial relevance of this work is the model can be used to theoretically determine the cutting power of a new cutting device based on the rupture modulus of the palm fronds other parameters and can be used to develop a new cutting tool to further improve the frond cutter for the oil palm harvesting and pruning.

MATERIALS AND METHODS

Establishment of Kinematics Model for Sawing Oil Palm Fronds

The oil palm frond is in general wide at the base and tapering to the end of the frond. In this work the cutting of the frond would start at the centre where the frond was the thickest and move through the apex of the triangle to the top of the frond which is the widest. The setup is as shown in *Figure 1a* where the circular saw is located at the bottom of the frond.

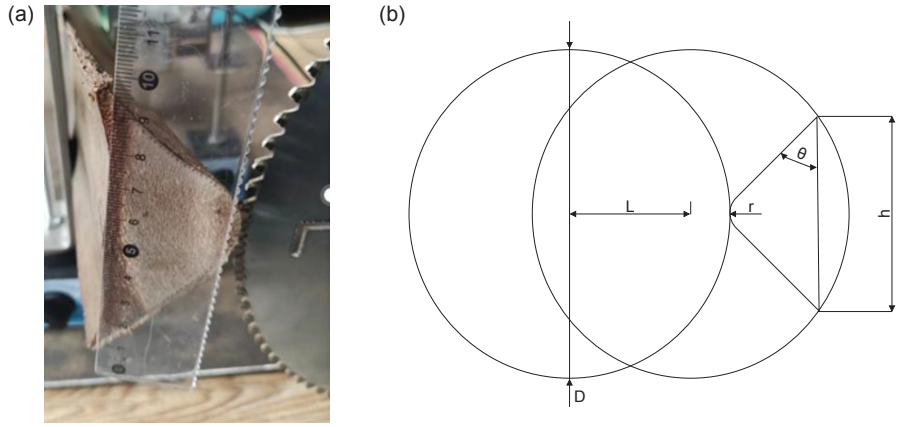

Figure 1. (a) Section of oil palm and (b) schematic diagram of sawing oil palm fronds.

The section can be regarded as an isosceles triangle with an obtuse angle and an arc top angle. It can be simplified as *Figure 1b*. The maximum width of the cutting cross section of h fronds, θ was the included angle of the fronds, and r was the fillet radius of the bottom edge of the fronds.

As shown in *Figure 1b*, assuming that the parameters to be solved are the total travel of the circular saw from the initial cutting position to the final cutting position (L), required time (t_1) and cutting area ($S_{Fronds\text{-}area}$) the Equations (1) to (4) are derived based on the geometry of the frond based on *Figure 1b*.

$$L = \frac{1}{2} \cdot h \cdot \tan\theta - \left(\frac{r}{\sin 45°} - r_e\right) + \left(\frac{D}{2} - \sqrt{\left(\frac{D}{2}\right)^2 - \left(\frac{h}{2}\right)^2}\right) \quad (1)$$

$$t_1 = \frac{L}{\mu} \quad (2)$$

$$= \frac{1}{u} \cdot \left[\frac{1}{2} \cdot h \cdot \tan\theta - (\sqrt{2}-1) \cdot r + \frac{D - \sqrt{D^2 - h^2}}{2}\right] \quad (3)$$

The area of the fronds cutting part:

$$S_{Fronds\text{-}area} = \frac{1}{2} \cdot h \cdot \tan\theta \cdot \left(\frac{h}{2}\right) - \left(r^2 - \frac{\pi \cdot r^2}{4}\right) \quad (4)$$

where D is the circular saw diameter, h is the maximum width of the cross section of the fronds, θ is the side angle of the fronds, r is the fillet radius of the bottom edge of the fronds, u is the feed rate of the tool.

Power Calculation Model for Sawing Oil Palm Fronds

Cutting feed power of sawing oil palm fronds. According to Hlásková *et al.* (2015), the mechanical process of material separation from the saw work piece (*i.e.*, chip formation) could be described as an orthogonal process (two-dimensional deformation). The forces acting on the tooth could be represented in the classical approach by Ernst and Merchant's force circle is shown in *Figure 2*.

F_a is the active force, F_c is the cutting force, F_f is the thrust force (passive), F_μ is the friction force on the rake face, F_N is the normal force to the rake face, $F_{T\phi}$ is the force required to shear the wood along the shear plane, $F_{N\phi}$ is the normal force on the shear plane, α_f is the clearance angle, ϕ_c is the shear angle, γ_f is the rake angle, and β_μ is the friction angle (Hlásková *et al.*, 2015).

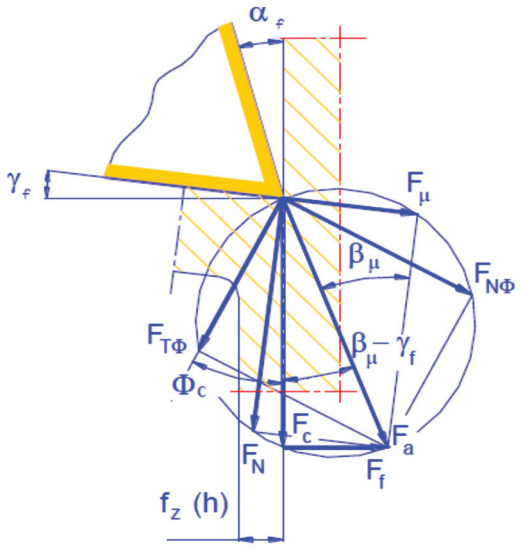

Source: Hlásková *et al.*, 2015.

Figure 2. Simplified cutting process model with Ernst and Merchant's force circle.

The cutting power for one saw blade during the cutting stroke of a sash gang saw, in which both chip momentum (Hlásková *et al.*, 2015) and a ploughing effect caused by tooth cutting edge dullness (Wang *et al.*, 2013) were disregarded, follows Equation (5).

The shear angle ϕ_c, for the necessary aim of this study, can be calculated for larger values of feed per tooth f_c with the Merchant's equation (because for large uncut chip values ϕ_c was constant) (Atkins, 2003) [Equation (6)].

$$\beta_\mu = \tan^{-1}(\mu) \tag{5}$$

$$\phi_c = (\pi/4) - (1/2)(\beta_\mu - \gamma_f) \tag{6}$$

μ is the friction coefficient of the cutting section of the oil palm fronds measured by the test. γ_f is the rake angle of the circular saw.

Sawing productivity f of the circular saw when sawing the work piece [Equation (7)].

$$f = \frac{S_{Fronds\text{-}area}}{t_1} = \frac{1/4 \cdot (h^2 \cdot \tan\theta + \pi \cdot r^2) - r^2}{\frac{1}{u} \cdot [\frac{1}{2} \cdot h \cdot \tan\theta - (\sqrt{2}\text{-}1) \cdot r + \frac{D - \sqrt{D^2 - h^2}}{2}]} \tag{7}$$

During sawing, the sawing deformation work per unit volume of the fronds to be cut is A [Equation (8)].

$$A = \frac{k(1+\cot\phi_c)(\sin\theta_1 - \sin\theta_2)}{(\theta_1 - \theta_2)\cos\bar{\alpha}} \approx k(1+\cot\phi_c) \tag{8}$$

k was the rupture modulus of the fronds, and test for Sampling Method according to (Intara *et al.*, 2013). ϕ_c is the shear angle when the circular saw is cutting.

The cutting feed power during the sawing process P_1 can be deduced through Equation (9).

$$P_1 \approx \frac{ABf}{10^6} = \frac{f(\vartheta + 0.0006D)A}{10^6} = \frac{f(\vartheta + 0.0006D) \cdot k(1+\cot\phi_c)}{10^6} \tag{9}$$

$$= \frac{[(h^2 \cdot \tan\theta + \pi \cdot r^2) - 4r^2] \cdot (\vartheta + 0.0006D) \cdot k(1+\cot\phi_c)}{\frac{4}{u} \cdot [\frac{1}{2} \cdot h \cdot \tan\theta - (\sqrt{2}\text{-}1) \cdot r + \frac{D - \sqrt{D^2 - h^2}}{2}]} \tag{10}$$

From the Equation 9 and 10, ϑ is the thickness of the tool (*mm*), ϕ_c is the shear angle when the circular saw is cutting (°), and D is the diameter of the tool (*m*).

Power required for bending work piece. When sawing the work-piece, saw tooth just touches the work-piece, the work-piece will produce bending deformation under the external force. The bending deformation energy will also consume part of the power. In the sawing process, the power consumed by the bending deformation of the work piece is P_2, therefore,

$$P_2 = \frac{U_{bend}}{5t_{bend}} \tag{11}$$

The P_2 is the bending deformation energy of the work piece. It is found that the value of P_2 is very small, almost zero and can be ignored.

Clamping saw power for sawing oil palm frond. In the process of sawing the workpiece, a slit was formed at the sawing position of the circular saw. The inner wall of the front limited the deformation of the circular saw during sawing. When the workpiece was sawed at a constant speed, the circular saw was subjected to the friction of the side wall of the slit, which inevitably consumed a certain amount of cutting work. The power P_3 consumed to overcome the friction is called the power of the saw clamp [Equation (12)].

$$P_3 = \frac{\mu V (\frac{f_d}{c})}{102} \tag{12}$$

where, V is the linear speed, μ is the friction coefficient of the cutting section of the oil palm fronds measured by the test, and c is the dynamic load factor of circular saw. f_d is the dynamic load amplitude of the circular saw (if V<2 mm/s, then f_d = 0.0006; if 2 mm/s<V<5 mm/s, then f_d = 0.0009; if 5 mm/s<V<10 mm/s, then f_d = 0.0015; and if V>10 mm/s, then f_d = 0.0028.). The final comprehensive cutting power of the oil palm fronds is as follows:

$$P_{total} = P_1 + P_2 + P_3 \tag{13}$$

The final cutting work result J can be obtained by multiplying the total power P_{total} required for circular saw cutting and the time t_1 required for cutting as Equation 13.

$$J = P_{total} \cdot t_1 \tag{14}$$

The method used in this study was an idealised cutting condition, which did not represent the frond in its natural state, but was most closely supported as a cantilever beam. The application of the weight of the frond at the free end reduced the friction power, as the bending moment of the frond weight helped to open up the cut part of the frond and reduced the normal force and the ensuing friction force on the radial cutter saw. However, the simplified support used in this study was easy to replicate by other researchers in order to obtain comparable cutting data. The same approach had been adopted in the study for static cutting force by Jelani *et al.* (1998).

Experimental Study

The experimental work was carried out in two different stages, the first stage was to characterise the frond properties in terms of the modulus of rupture and the friction coefficient between the frond and the circular saw. These were the required parameters for the cutting model and the second stage was the measurement of the cutting force and power of the circular saw when cutting the fronds.

Experimental measurement of the frond rupture modulus* (k) *and friction coefficient. In order to determine the rupture modulus of the frond, the specimen was prepared from the fronds of an eight year old oil palm tree obtained from a plantation in Yunnan, China. These specimens were then tested in the tensile test equipment (Zwick, CTM tensile test equipment). Samples were prepared and tested according to the storage period from fresh to 10, 20, and 30 days. Three sets of appropriately sized samples (*Figure 3*) were selected. The weight of each fresh sample was recorded, and the average weight (W) was calculated. After placing the samples for 10 days, the average weight (W_1) was recorded. After a natural resting period of 20 days, the average weight (W_2) was recorded. Similarly, after a natural resting period of 30 days, the average weight (W_3) was recorded. The percentage of moisture content W_c in the oil palm fronds were calculated using Equation (15).

$$W_c = \frac{W - W_{1or2or3}}{W} \times 100\% \quad (15)$$

The moisture content of the specimens was determined to be 58%, 43%, 31% and 12% respectively. The samples were prepared such that they were free from burr and stored in the cupboard for airing under natural ventilation, and the dimensions of specimens were shown in the *Figure 3* below.

Figure 3. The samples of fronds.

The tensile test was carried out on the specimen as shown in *Figure 4*. The load was applied on the specimen at 2 min/mm speed until fracture where the computer automatically records the required breaking force of the specimen.

Figure 4. The measurement test of rupture modulus.

***Measurement of the friction coefficient* (μ).** The sample for the friction coefficient test was made in specimen with the width of 100 mm. The inclined angle technique used, which consisted of a high-speed camera analysis system, a high-speed camera, LED fill light, protractor, and friction coefficient measuring slope meter, and the sliding surface was made of 65 Mn tool steel to best represent the circular saw.

The sliding distance and time of the test piece on the friction coefficient tester were calculated by high-speed camera and then the sliding acceleration of the test piece was calculated. The dynamic friction coefficient of the test piece on the 65 Mn tool steel surface can be calculated according to the force balance equation of the test piece on the slope. By utilising a high-speed camera to capture the displacement of both specimen and the 65 Mn tool steel at various time points, we proceed to calculate the dynamic friction coefficient. The specific procedural framework for elucidating this process can be delineated as follows.

As shown in *Figure 5*, the shooting frequency was set to 120 pictures/s under the high-speed shooting state, so the sliding time of the test piece in each frame was 8.33 ms. The sliding time of the test piece can be obtained by calculating the difference between the number of frames between the start position and the end position and the sliding distance of the test piece can be measured. The dynamic friction coefficient (μ) of the test piece

on the surface of 65 Mn tool steel can be calculated by Equation (16).

$$\mu_k = \frac{2 \cdot S}{g \cdot \cos\theta' \cdot t_2^2} \tag{16}$$

where, θ' is the inclination angle of the inclinometer, S is the distance travelled between two successive photos and t_2 is the time lapse between the frames of the photos.

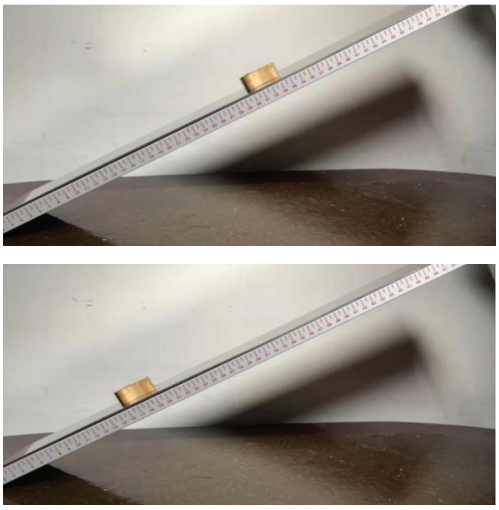

Figure 5. Determination process of friction coefficient from two successive photos.

Measurement of power of circular saw when cutting frond. The power of the circular saw motor was measured by the multi-function power meter. The multi-function power meter transmitted the data to the Personal Computer (PC) through the serial port data converter. The PC stored the data in real time through the serial port debugging software, and then converted it into a curve chart through Matlab software to obtain the power time domain diagram in the cutting process. *Figure 6* showed the ART data acquisition system for multi-function power meter to measure the power of the three-phase motor (ABB - 2.2kw - 4P - asynchronous motor). Three current sensors were clamped to each wire as shown in *Figure 6* respectively in order to measure the current through the U, V, W lines of the three-phase supply.

The ART was powered by voltage and these were then connected to the motor three-phase voltage, and voltage data of the motor was directly collected by ART. The 485 to 232 serial port data converters connected the multi-functional power instrument with the PC host. The multi-functional power instrument was the serial port of 485, and the PC host was the serial port of 232 (Xie, 2019) and this was combined with Modbus communication protocol for data conversion and acquisition of the PC. The data transmitted from multi-function power meter to PC was hexadecimal data, which was converted to decimal data through Modbus protocol of serial port debugging software.

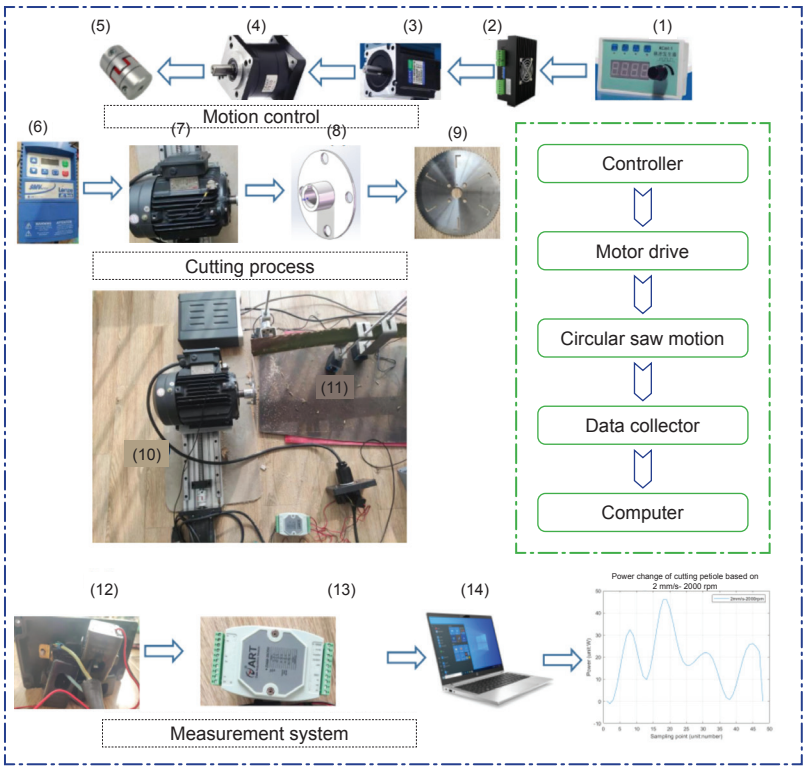

Note: (1) - Controller; (2) - Step driver; (3) - Stepper motor; (4) - Decelerator; (5) - Coupling; (6) - Frequency transformer; (7) - AC motor; (8) - Cutter coupling; (9) - Circular saw; (10) - Feed assembly; (11) - Fixed structure; (12) - Sensor; (13) - Acquisition instrument; (14) - Computer.

Figure 6. The overall setup of the cutting power measurement.

Cutting test of oil palm fronds was conducted based on the oil palm comprehensive cutting test bench. The test conditions were the (1) feed rate at 2, 4, 8 and 12 mm/s, (2) rotation speed of the circular saw at 1,000-2,600 rpm. The data sets obtained were used to verify the value of power consumption obtained from the model.

The Process Diagram for Model Establishment and Validation

In summary, the establishment and validation of the cutting model for oil palm fronds are demonstrated through three specific steps, as illustrated in *Figure 7*.

RESULTS AND DISCUSSION

Fronds Characterisation

Rupture modulus. *Figure 8* below shows the rupture modulus as a function of moisture content. The normal drying of the specimens produces moisture content of 12%-58% and the results of the fracture modulus show that the strength of the frond increases almost linearly as the moisture content is reduced. The maximum rupture modulus is 43 MPa at 12% moisture and the lowest rupture modulus 28 MPa as in *Figure 8*. It is well known that woody specimens have similar regular pattern and increases the fracture toughness as the moisture content reduces. The fracture modulus of oil palm or king palm fronds ranged from 19-44 MPa at different water content (Chen, 2012; Wang, 2016; Wu, 2013).

The results of regression analysis *Figure 8* shows that $P<0.05$ the moisture content has a significant impact on the rupture modulus k. In other words, the significant linear relationship between rupture modulus k and moisture content has been verified. The tissue structure of oil palm fronds with different moisture content has a great impact on the variation of the required rupture force, and there is a linear correlation between the variation of oil palm fronds rupture modulus k and the moisture content of fronds. The moisture content continues to decrease with the extension of storage time, which causes to more serious fibrillation of fronds. Lower moisture content will lead to the ability to resist fracture (rupture modulus k) is enhanced. Lin (2012) developed rupture modulus model for wood species using moisture content (MC) as parameters. It seemed reasonable to expect that the main force would decrease with increased MC.

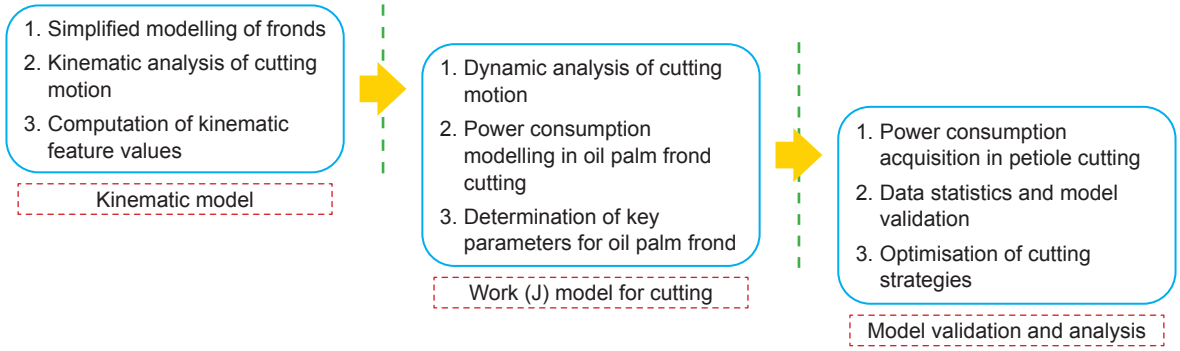

Figure 7. The process diagram for model establishment and validation.

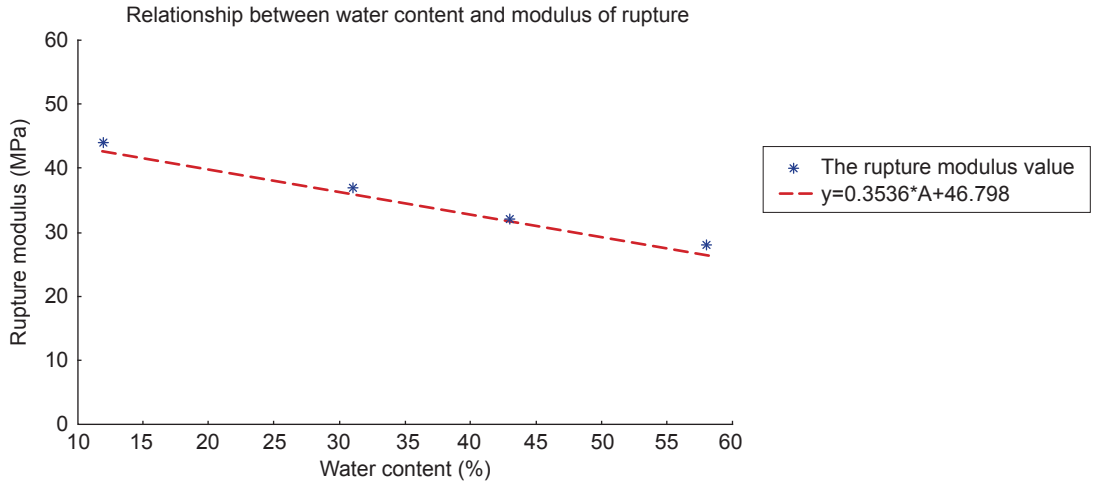

Figure 8. Effect of moisture content on the modulus of rupture of oil palm frond.

Friction coefficient of frond and circular saw. The critical angle of sliding of the test piece on the inclined plane was tested and was determined to be at 30°. The test was conducted for angles above the critical angle in order to find the variation of friction coefficient with the speed and the angle of inclination of up to 50° was tested for. The results are shown in *Figure 9* below. In this figure the general trend is that the friction, which coefficient is reducing with the sliding speed and this compares well with the trend of static friction which is higher than the kinetic friction as generally observed. The friction coefficient is highest at 0.55 at 0.75 m/s sliding speed and lowest at 0.41 at the sliding speed of 1.1 m/s is shown in the *Figure 9*. The trend of the data observed here correlates well with the data obtained elsewhere on wood specimen (Guan *et al.*, 1983; McMillin *et al.*, 1970; Murase *et al.*, 1978) for the case where the wood moisture content was large, the friction coefficient decreased with the increase of sliding speed. With the increase of sliding speed, the bond stability becomes weaker, and the friction coefficient also decreases. The moisture content of fresh oil palm frond tested here was more than 50%, belonging to high moisture content (Li & Zhang, 2018). The results obtained here is to be used as a guideline in the modelling of the cutting process.

Cutting Work of Circular Saw when Cutting Fronds

Figure 10 shows the different cutting power for several rotational speed of the circular saw, the Y-axis coordinate represents the cutting work (J) between the rotation speed and the cutting work under the working condition of the circular saw cutting feed rate of 2, 4, 8 and 12 mm/s. The cutting work was directly related to the rotation speed and feed rate. The cutting work had a linear function to rotation speed. Guedes *et al.* (2020), Li *et al.* (2022) and Nasir *et al.* (2018) studied the power consumption of cutting different types of wood (pine, tobacco fronds, ash *etc.*) using a circular saw. They also concluded that the power consumption increases linearly with the increase in the rotational speed of the circular saw. From the perspective of kinematic transmission laws, the power consumption model equation and experimental results are consistent with existing research results. Xie (2019) studied the power consumption of sugarcane cutting within the range of tool speed conditions of 250-500 rpm. It was found that the power consumption required for complete cutting of sugarcane falls within the range of 400-800 J.

The experimental data and research (*Figure 10*) results show that large gap between the individual data and the prediction results does not affect the final significance determine, which may be caused by the vibration of the circular saw and the uneven distribution of the texture of the cut body (Porankiewicz *et al.*, 2011). The data for the cutting work has a certain degree of dispersion, which is a normal phenomenon in the test. In general, it can be seen that there is a significant relationship between the test data and cutting work model for the oil palm fronds under the condition of rotation speed from 1,000-2,600 rpm and the feed rate of 2, 4, 8 and 12 mm/s. The distribution correlation coefficient ranges 0.72-0.91, ranges 38.12-144.35 and $P<0.05$. The red dotted line is the theoretical line from the model developed (Equation 13) and the correlation is good with R-square values, F statistic values and P values for the cases investigated. The significance of the model is statistically robust. It can be said the cutting model developed is validated.

The model developed here is based on a limited sample size. Increasing the sample size will effectively diminish the errors resulting from coupling effects. There is also a need to investigate the tooth profile which can strongly affect the

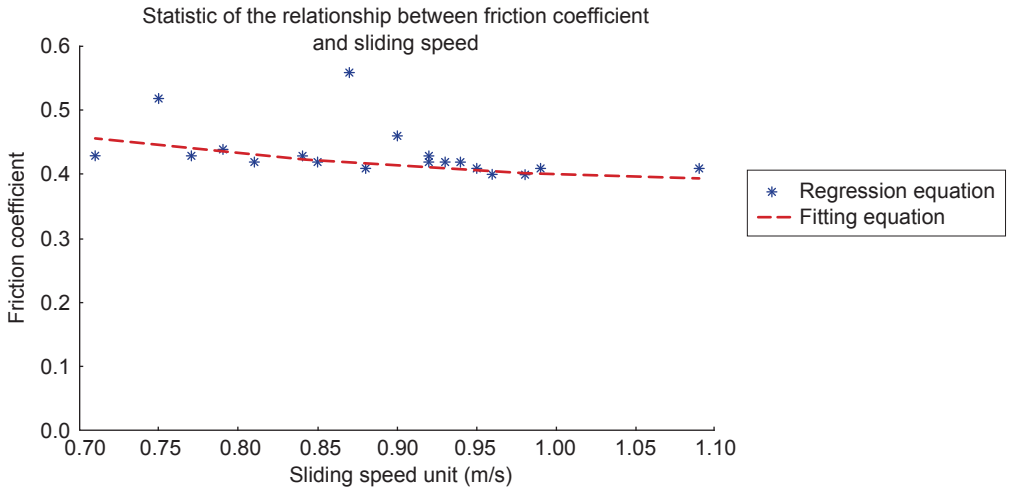

Figure 9. Variation of friction coefficient of oil palm frond with sliding speed.

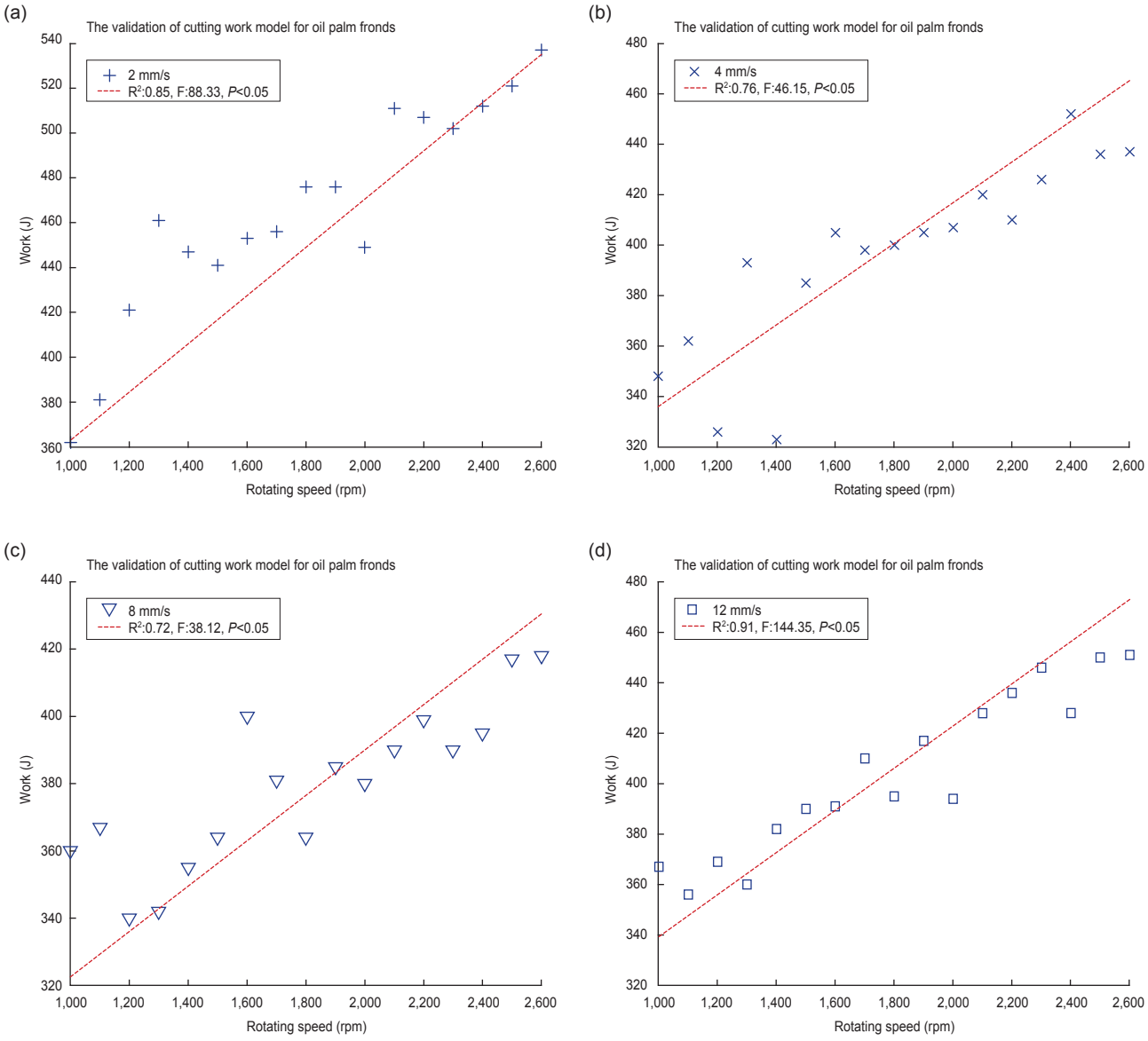

Figure 10. Theoretical cutting work (red line) and experimental reading (+,×,▽, □) for various feed rate (a) 2 mm/s, (b) 4 mm/s, (c) 8 mm/s and (d) 12 mm/s respectively.

cutting force and the effect of the angle of the saw relative to the frond fibre orientation as the current study only consider cutting perpendicular to the fibre of the frond. It would also be appropriate to study the theoretical cutting model for the existing sickle type harvester and the chisel type harvester. This can enable the resulting models to be compared with the radial saw cutter investigated here.

Optimisation of the Cutting Parameters

The model of the circular saw cutting process can now be used to determine the effect of the operating parameters on the work done for the cutting process. In this study, the range of the cutting parameters considered are 1-12 mm/s of feed rate and 1,000-3,000 rpm rotation speed of the circular saw. The results of those are shown in the *Figure 11* below. The energy consumed reduces linearly with the reduction of circular saw rotation speed and the variation of the energy consumed with the feed rate cannot be simply described as linear. When the feed rate of the circular saw increases from 1-3 mm/s, the cutting work decreases sharply. When the feed rate of the circular saw reaches 5 mm/s, the cutting work reaches the first peak bottom. When the feed rate of the circular saw increases from 6-12 mm/s, the cutting work of the cutting reaches the second peak bottom, which is the lowest point of energy consumption. When the feed rate of circular saw is 10 mm/s, the cutting work is the minimum. Within the range investigated, the minimum energy consumed is at circular saw rotation speed of 1,000 rpm and 10 mm/s feed rate.

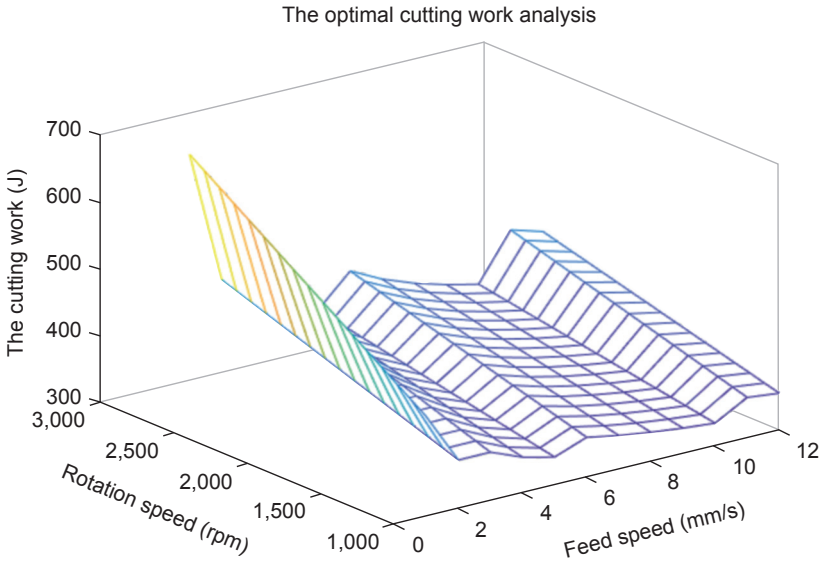

Figure 11. Analysis of optimal cutting work based on different working conditions.

Challenges and Future Work

The model developed here is based on a limited sample size. In particular, the age of the fronds and also the different size. There is also a need to investigate the tooth profile which can strongly affect the cutting force and the effect of the angle of the saw relative to the frond fibre orientation as the current study only consider cutting perpendicular to the fibre of the frond. It would also be appropriate to study the theoretical cutting model for the existing sickle type harvester and the chisel type harvester. This can enable the resulting models to be compared with the radial saw cutter investigated here.

CONCLUSION

Experimentally determined characteristics of the fronds used in this study are the rupture modulus (28-43 MPa) and friction coefficient for different sliding speed (0.41-0.55 at 0.75-1.10 m/s) measured at moisture content of (12%-58%). A frond cutting model was developed based on the Ernst and Merchant's force circle and the energy consumption based on the cutting power and clamping power expenditure. The energy consumption of the circular saw from the model is verified with the measured cutting energy of (330-540 J) at 1,000-2,600 rpm and feed rate of 2-12 mm/s ($0.72<R^2<0.91$, $P<0.05$). The validated cutting energy equation is used in the optimisation of the cutting process of a 100 mm base wide of an oil palm frond resulting in the minimum cutting energy of 330 J for rotational speed of 1,000 rpm and feed rate of 10 mm/s.

ACKNOWLEDGEMENT

The authors are grateful to the insightful comments suggested by the editor and the anonymous reviewers.

REFERENCES

Abbood, S. M. (2020). Effect of moisture ratio and cutting angles on force required to cut date palm fronds. *Biochemical and Cellular Archives, 20*(1), 1995–1997. https://doi.org/10.35124/bca.2020.20.1.1995

Abbood, S. M., Abbood, M. R., & Jasim, A. A. (2018). Manufacturing and testing of date palm vibration motorized fronds cutter. *Iraqi Journal of Agricultural Sciences, 49*(3), 763–773.

Atkins, A. (2003). Modelling metal cutting using modern ductile fracture mechanics: Quantitative explanations for some longstanding problems. *International Journal of Mechanical Sciences, 45*(2), 373–396. https://doi.org/10.1016/s0020-7403(03)00040-7

Chen, L. (2012). *Research on multi-scale model and mechanical properties of branching system of the family Palmae* (Master's thesis). South China University of Technology, Guangzhou.

Chu, H. (2017). *Design and experimental research of cutting key device for collecting potato stalk* (Doctoral dissertation). China Agricultural University.

Dong, R. (2017). *Simulation and experimental study on cutting process of silage corn harvesting header* (Master's thesis). Jilin University.

Eliçin, A. K., Sessiz, A., & Pekitkan, F. G. (2019). Effect of various knife type, cutting angle and speed on cutting force and energy of grape cane. *European Journal of Science and Technology*, 519–525. https://doi.org/10.31590/ejosat.532914

Gao, Z. (2016). *The bionic design of circular saw blade for metal cutting* (Master's thesis). Jilin University.

Guan, N., Thunell, B., & Lyth, K. (1983). On the friction between steel and some common swedish wood species. *European Journal of Wood and Wood Products*, *41*(2), 55–60. https://doi.org/10.1007/bf02612232

Guedes, T. O., Moreira da Silva, J. R., Hein, P. R. G., & Ferreira, S. C. (2020). Cutting energy required during the mechanical processing of wood species at different drying stages. *Maderas. Ciencia y Tecnología, 22*(4), 477–482. https://doi.org/10.4067/S0718-221X2020005000406

Hlásková, L., Orlowski, K. A., Kopecký, Z., & Jedinák, M. (2015). Sawing processes as a way of determining fracture toughness and shear yield stresses of wood. *BioResources, 10*(3), 5381–5394. https://doi.org/10.15376/biores.10.3.5381-5394

Intara, Y. I., Mayulu, H., & Radite, P. (2013). Physical and mechanical properties of oil palm frond and stem bunch for developing pruner and harvester machinery design. *International Journal of Science and Engineering, 4*(2), 69–74. https://doi.org/10.12777/ijse.4.2.2013.69-74

Jasim, A. A., Abbood, M. R., & Abbood, S. M. (2017). Effect of knives type on some operational characteristics for a locally assembled motorized vibration cutter used for date palm fronds pruning. *International Journal of Environment, Agriculture and Biotechnology, 2*(4), 1597–1600. https://doi.org/10.22161/ijeab/2.4.19

Jelani, A. R., Ahmad, D., Hitam, A., Yahya, A., & Jamak, J. (1998). Force and energy requirements for cutting oil palm frond. *Journal of Oil Palm Research, 10*(2), 10–24.

Jelani, A. R., Ahmad, D., Hitam, A., Yahya, A., & Jamak, J. (1999). Reaction force and energy requirement for cutting oil palm fronds by spring powered sickle cutter. *Journal of Oil Palm Research, 11*(2), 114–122.

Li, C., Zhang, H., Wang, Q., & Chen, Z. (2022). Influencing factors of cutting force for apple tree branch pruning. *Agriculture, 12*(2), 312. https://doi.org/10.3390/agriculture12020312

Li, P., Wang, S., Xiong, B., Tang, X., Tong, Y., Gao, S., Wen, S., Huang, M., Duan, Z., & Chen, Q. (2022). Laser cutting tobacco slice experiment: Effects of cutting power and cutting speed. *Open Physics, 20*(1), 977–983. https://doi.org/10.1515/phys-2022-0034

Li, W., & Zhang, Z. (2018). Research progress of friction behaviour in wood cutting. *China Wood Industry, 32*(6), 23–27. https://doi.org/10.19455/j.mcgy.20180606

Lin, X. (2012). *Calculation research on force and energy parameters of the metal sawing process of circular sawing machine* (Master's thesis). Central South University, Hunan.

McMillin, C. W., Lemoine, T. J., & Manwiller, F. G. (2007). Friction coefficient of Oven-Dry spruce pine on steel, as related to temperature and wood properties. *Wood and Fiber Science, 2*(1), 6–11. https://wfs.swst.org/index.php/wfs/article/download/681/681

Meijide, A., Röll, A., Fan, Y., Herbt, M., Niu, F., Tiedemann, F., June, T., Rauf, A., Hölscher, D., & Knohl, A. (2017). Controls of water and energy fluxes in oil palm plantations: Environmental variables and oil palm age. *Agricultural and Forest Meteorology, 239*, 71–85. https://doi.org/10.1016/j.agrformet.2017.02.034

Meng, Y., Wei, J., Wei, J., Chen, H., & Cui, Y. (2018). An ANSYS/LS-DYNA simulation and experimental study of circular saw blade cutting system of mulberry cutting machine. *Computers and Electronics in Agriculture, 157*, 38–48. https://doi.org/10.1016/j.compag.2018.12.034

Murase, Y. (1978). Effect of surface roughness of steel and wood variables on repeated friction between wood and steel. *Japan Wood Research, 24*(5), 865–872.

Nasir, V., Mohammadpanah, A., & Cool, J. (2018). The effect of rotation speed on the power consumption and cutting accuracy of guided circular saw: Experimental measurement and analysis of saw critical and flutter speeds. *Wood Material Science and Engineering, 15*(3), 140–146. https://doi.org/10.1080/17480272.2018.1508167

Porankiewicz, B., Axelsson, B., Grönlund, A., & Marklund, B. (2011). Main and normal cutting forces by machining wood of Pinus sylvestris. *BioResources*, *6*(4), 3687–3713. https://doi.org/10.15376/biores.6.4.3687-3713

Suryanto, N. H., Ahmad, N. D., Yahya, N. A., Akande, N. F. B., & Syahrita, N. K. (2009). Technical note: Cutting tests of oil palm empty fruit bunches. *Transactions of the ASABE*, *52*(3), 723–726. https://doi.org/10.13031/2013.27388

Wang, H., Chang, L., Ye, L., & Williams, J. G. (2013). Micro-cutting tests: A new way to measure the fracture toughness and yield stress of polymeric nanocomposites. *Proceedings of the 13th International Conference on Fracture*, 1–12. https://www.gruppofrattura.it/ocs/index.php/ICF/icf13/paper/viewFile/11399/10778

Wang, N. (2016). *Multi-scale modeling of royal palm tissue and the bionic applications based on its tissue structure* (Doctoral dissertation). South China University of Technology, Guangzhou.

Wu, H. (2013). *Research on structure and mechanical property of the family Palmae and bionic design of wind turbine* (Master's thesis). South China University of Technology, Guangzhou.

Xie, L. (2019). *Design and parameter optimization of stalk chopping, leaf stripping and top breaking devices for sugarcane harvester* (Doctoral dissertation). Zhejiang University.